Journal of Cardiovascular Magnetic Resonance (2005) **7,** 595–602

ISSN: 1097-6647 print / 1532-429X online
DOI: 10.1081/JCMR-200060624

Taylor & Francis
Taylor & Francis Group

VENTRICULAR FUNCTION

Improved quantification of left ventricular volumes and mass based on endocardial and epicardial surface detection from cardiac MR images using level set models

CRISTIANA CORSI, PH.D.,[1,2] CLAUDIO LAMBERTI, M.S.,[1] ORONZO CATALANO, M.D.,[3] PETER MACENEANEY, M.D.,[2] DIANNA BARDO, M.D.,[2] ROBERTO M. LANG, M.D.,[2] ENRICO G. CAIANI, PH.D.,[4] and VICTOR MOR-AVI, PH.D.[2,*]

[1]*Department of Electronics, Computer Science and Systems, University of Bologna, Bologna, Italy*
[2]*University of Chicago Medical Center, Chicago, Illinois, USA*
[3]*Salvatore Maugeri Foundation, Pavia, Italy*
[4]*Dipartimento di Bioingegneria, Politecnico di Milano, Milan, Italy*

Purpose. The reproducibility of left ventricular (LV) volume and mass measurements based on subjective slice-by-slice tracing of LV borders is affected by image quality, and volume estimates are biased by geometric modeling. The authors developed a technique for volumetric surface detection (VoSD) and quantification of LV volumes and mass without tracing and geometric approximations. The authors hypothesized that this technique is accurate and more reproducible than the conventional methodology. *Methods.* Images were obtained in 24 patients in 6 to 10 slices from LV base to apex (GE 1.5 T, FIESTA). Volumetric data were reconstructed, and endocardial and epicardial surfaces were detected using the level set approach. LV volumes were obtained from voxel counts and used to compute ejection fraction (EF) and mass. Conventional measurements (MASS Analysis) were used as a reference to test the accuracy of VoSD technique (linear regression, Bland-Altman). For both techniques, measurements were repeated to compute inter- and intra-observer variability. *Results.* VoSD values resulted in high correlation with the reference values (EDV: r = 0.98; ESV: r = 0.99; EF: r = 0.91; mass: r = 0.98), with no significant biases (8 ml, 5 ml, 0.2% and −9 g) and narrow limits of agreement (SD: 13 ml, 10 ml, 6% and 9 g). Inter-observer variability of the VoSD technique was lower (range 3 to 5%) than that of the reference technique (5 to 11%; $p < 0.05$). Intra-observer variability was also lower (1 to 3% vs. 7 to 10%; $p < 0.05$). *Conclusion.* VoSD technique allows accurate measurements of LV volumes, EF, and mass, which are more reproducible than the conventional methodology.

Key Words: Global ventricular function; Ventricular mass; Magnetic resonance imaging; Computer analysis

1. Introduction

Cardiac magnetic resonance imaging (CMRI) is the standard for left ventricular (LV) volume, ejection fraction (EF), and mass measurements (1–3). However, LV volumes are routinely obtained using manual or semi-automated tracing of LV borders on multiple 2D slices and computations based on disk area summation approximation. Understandably, the reproducibility of this subjective and experience-dependent methodology is limited when endocardial definition is sub-optimal, as sometimes occurs near the apex. Moreover, the use of fixed slice thickness for disk summation in segments where the endocardium is not perpendicular to the imaging plane together with the use of fixed number of slices throughout the cardiac cycle, without taking into account systolic longitudinal shortening, may bias volume measurements. Accordingly, our aim was to develop an alternative technique for fast and objective quantification of LV volumes, EF, and mass, with minimal user interaction and no need for geometric modeling. To achieve these goals, we based our approach on volumetric reconstruction followed by surface detection (VoSD) in the 3D domain and by direct calculation of LV volumes, EF, and mass.

The level-set methods have been shown to provide accurate boundary detection in 2D and 3D echocardiographic images (4–6). We hypothesized that with the superior quality of MR images, this approach could be effectively applied to volumetric data reconstructed from these images. We tested this hypothesis by comparing the results of VoSD technique with LV volume, EF, and mass values obtained by the conventional methodology. We also tested the hypothesis that the VoSD technique might be more reproducible than the conventional methodology.

Received 8 October 2004; accepted 14 February 2005.
*Address correspondence to Victor Mor-Avi, Ph.D., University of Chicago Medical Center, 5841 S. Maryland Ave., Chicago, IL 60637, USA; Fax: (773) 702-1034; E-mail: vmoravi@medicine.bsd.uchicago.edu

2. Methods

2.1. *Study design*

Twenty-four consecutive patients (16 males, 8 females; age: 53 ± 17 years) referred for CMRI studies were recruited into the study, including 6 patients with normal LV size and function, 3 patients with coronary artery disease, 5 with dilated cardiomyopathy, 4 with hypertrophic cardiomyopathy, 2 with valvular disease, 2 with aortic abnormalities, and 2 with other cardiac pathologies. To establish the accuracy of the newly developed VoSD technique, images were analyzed using both the VoSD procedure and the conventional technique, which was used as a reference for comparisons. In a subgroup of randomly selected 12 patients, all measurements were repeated twice to assess the reproducibility of both techniques by calculating their intra- and inter-observer variability. For each technique, the intra-observer variability was studied by blindly reanalyzing the images by the same investigator at least one week later, and the inter-observer variability was studied by blindly reanalyzing the images by a second investigator. All tracings were performed by two experienced investigators, who had previously analyzed at least 100 CMRI studies. The investigators were blinded to all prior measurements.

2.2. *Image acquisition*

CMRI data were obtained using a 1.5 Tesla scanner (General Electric, Milwaukee, Wisconsin) with a phased-array cardiac coil. Electrocardiogram-gated localizing spin-echo sequences were used to identify the long-axis of the heart. Steady-state free precession (FIESTA) dynamic gradient-echo mode was then used to acquire images during breath-hold. Cine-loops were obtained in 6 to 10 short-axis slices, from the atrio-ventricular ring to the apex (9 mm slice thickness, no gaps) with a temporal resolution of 20 frames per cardiac cycle.

2.3. *Image analysis: reference technique*

Images were analyzed on a Sun workstation using commercial software (MASS Analysis, General Electric). Initially, LV slices were selected for analysis beginning with the highest

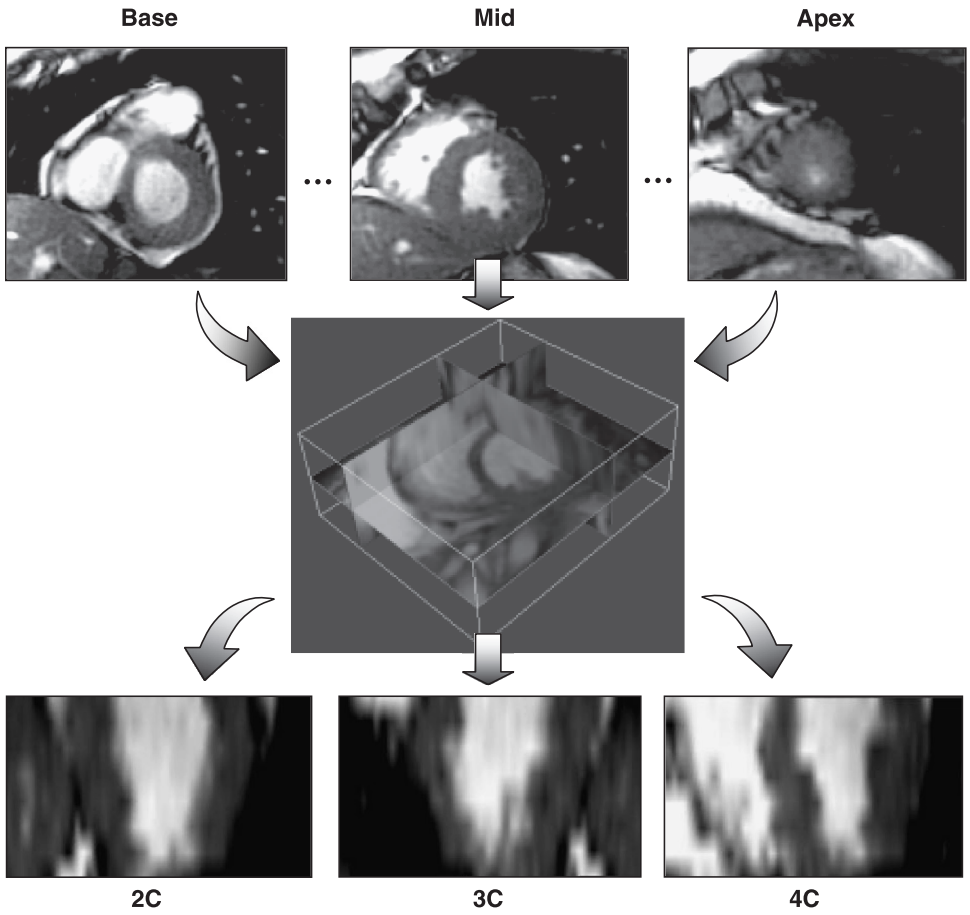

Figure 1. 3D reconstruction of a single CMRI dataset from a stack of short axis slices obtained at end-systole (top panels). A compact orthogonal view of the reconstructed 3D dataset (middle panel) allows on-line, interactive cross-sectioning and visualization of any arbitrary imaging plane. An example of 2-, 3- and 4-chamber views extracted from the volumetric dataset is shown below (bottom panels).

basal slice where the LV outflow tract was not visible and ending with the lowest apical slice where the LV cavity was visualized. In every slice, LV endocardial contours were traced semi-automatically frame-by-frame, with the papillary muscles included in the LV cavity, and manually corrected when necessary to optimize the boundary position. Then, ventricular volume was computed throughout the cardiac cycle using a disk-area summation method (modified Simpson's rule). End-diastolic (EDV) and end-systolic volumes (ESV) were determined as the maximum and minimum LV cavity volume reached during the cardiac cycle. These LV volumes were used to compute the EF as 100*(EDV − ESV)/EDV. Epicardial boundaries were then semi-automatically traced at end-diastole in each slice. LV mass was then computed as the difference between end-diastolic epicardial and endocardial volumes times the mass density constant (1.05 g/cc).

2.4. *Image analysis: VoSD technique*

The CMRI datasets were then analyzed using custom software, which allows ventricular surface detection using the level set approach (4–6). This method uses an implicit representation of curves in the form of a partial differential equation to track boundaries without geometrical assumptions or a priori shape knowledge.

First, a fully automated 3D reconstruction of the volumetric data was performed from the short-axis slices (Fig. 1). For each frame, a 3D dataset was generated using trilinear interpolation, while taking into account slice thickness, the number of slices, and the spacing between them. This resulted in a dynamic representation of the entire heart. This dynamic display was used to select end-diastolic and end-systolic frames, which were visually determined as the largest and smallest LV cavities in the 3D space.

Subsequently, semi-automated endocardial surface detection (Fig. 2) was performed separately for the end-diastolic and end-systolic frames. For surface initialization, a small number of short-axis planes (4 to 6) from apex to base were arbitrarily selected from the 3D dataset, and a number of points (6 to 12) were manually selected in each of these planes. To be consistent with the reference technique, the papillary muscles were included within the LV cavity and the aortic outflow tract was excluded. The selected points were connected by straight lines to define a polygon roughly representing the endocardial boundary. For each polygon, a signed distance function was calculated (7), and a rough surface corresponding to the endocardium was computed using linear interpolation of the signed distance functions. This surface was then used as the initial condition for the level-set partial differential equation, which guided the evolution of this surface within the volumetric dataset towards the endocardium. The partial differential equation guides the evolution of an initial surface under the constraints of two forces: 1) an interface tension force that depends on the curvature of the evolving surface and has a regulating effect and 2) a force that attracts this surface towards the image boundaries. The surface evolution reaches a steady-state

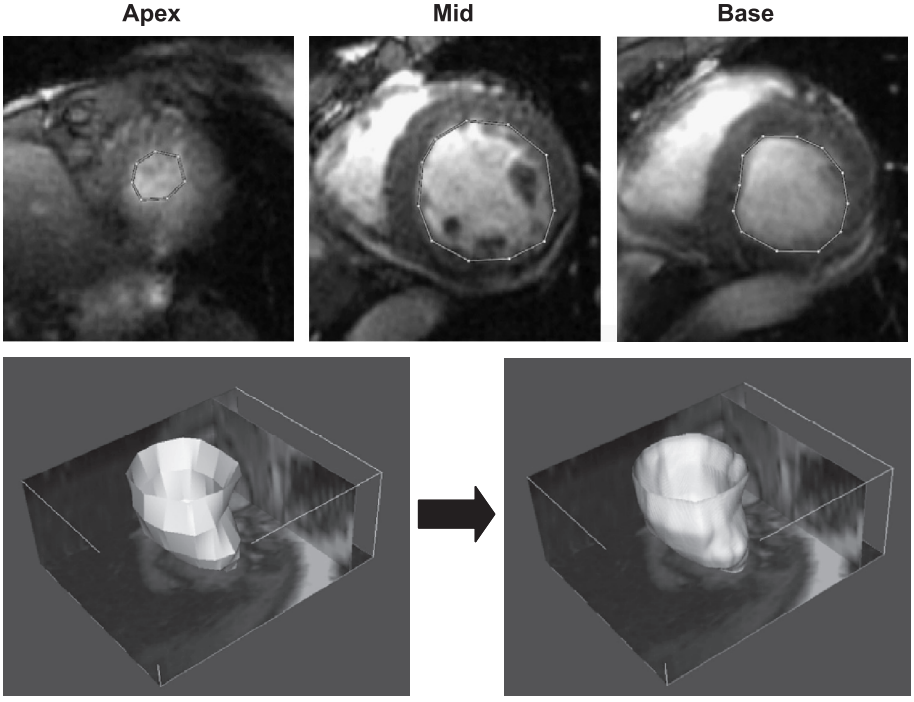

Figure 2. Example of manually initialized LV endocardial boundaries in three short-axis planes at end-diastole (top panels). Initial surface (bottom, left) and final endocardial surface (bottom, right) obtained by the VoSD technique.

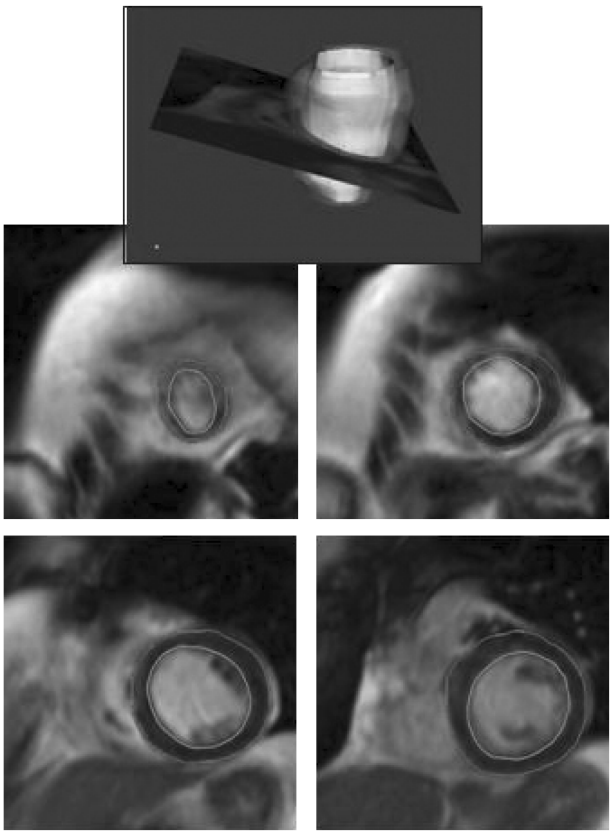

Figure 3. Superimposing of the detected endo- and epicardial surfaces on the volumetric data allows verification of the correctness of the detection in any arbitrary cross-sectional plane (top). Example of surface verification in multiple short-axis slices from the apical to the most basal slices is shown below (bottom panels).

solution when the two terms that reflect these forces balance each other. When the solution of the differential equation converged, the resultant final surface was used to represent the endocardium, and LV volume was calculated as the number of voxels within the detected surface. In addition, EF was calculated from EDV and ESV according to the same formula used for the reference technique.

Epicardial surface was detected only in the end-diastolic frame, following the same surface detection procedure, including the manual initialization of a small number of points. To verify the correctness of the endo- and epicardial surface detection, both surfaces were superimposed on the volumetric data (Fig. 3), which allowed cross-sectioning in any arbitrary plane and corrections of the initial points when necessary. After having the position of the endo- and epicardial surfaces confirmed in multiple cross-sectional planes, the end-diastolic epicardial volume was calculated as voxel count inside the detected epicardial surface. From the calculated end-diastolic endo- and epicardial volumes, LV mass was obtained according to the same formula used for the reference technique.

2.5. *Statistical analysis*

For each patient, VoSD measurements of LV EDV, ESV, EF, and mass were compared with the values derived by the reference technique using linear regression and Bland-Altman analyses. Paired *t*-test versus null values was applied to verify the significance of the bias. For each measured parameter, intra-observer variability of the reference technique and the VoSD technique were calculated as the absolute difference between the repeated measurements by the same investigator

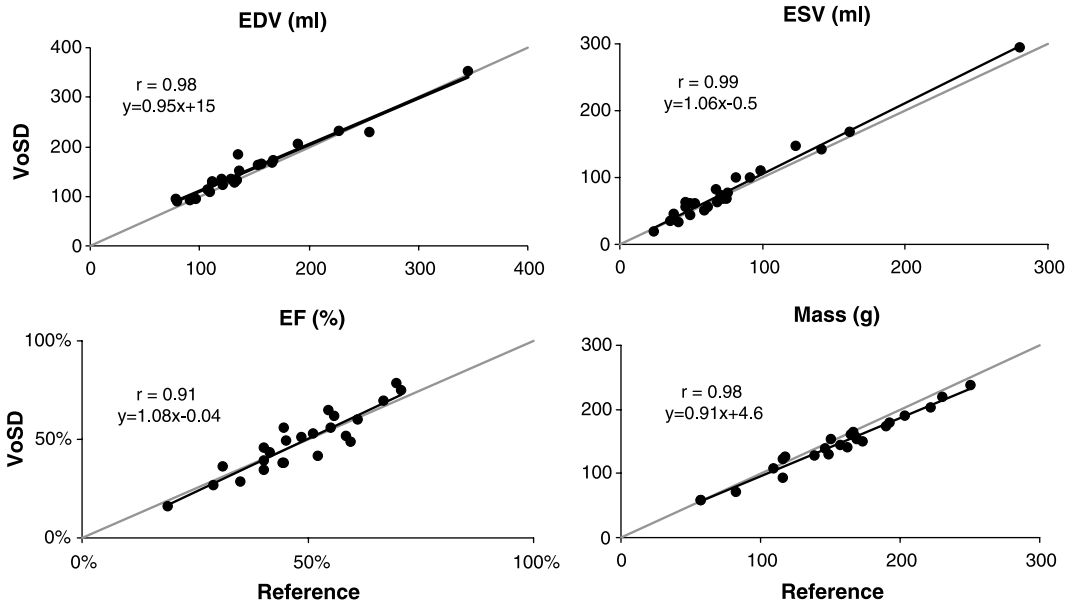

Figure 4. Linear regression analysis for LV EDV, ESV, EF, and mass obtained by the VoSD technique compared to the standard reference technique. Identity lines are shown in gray.

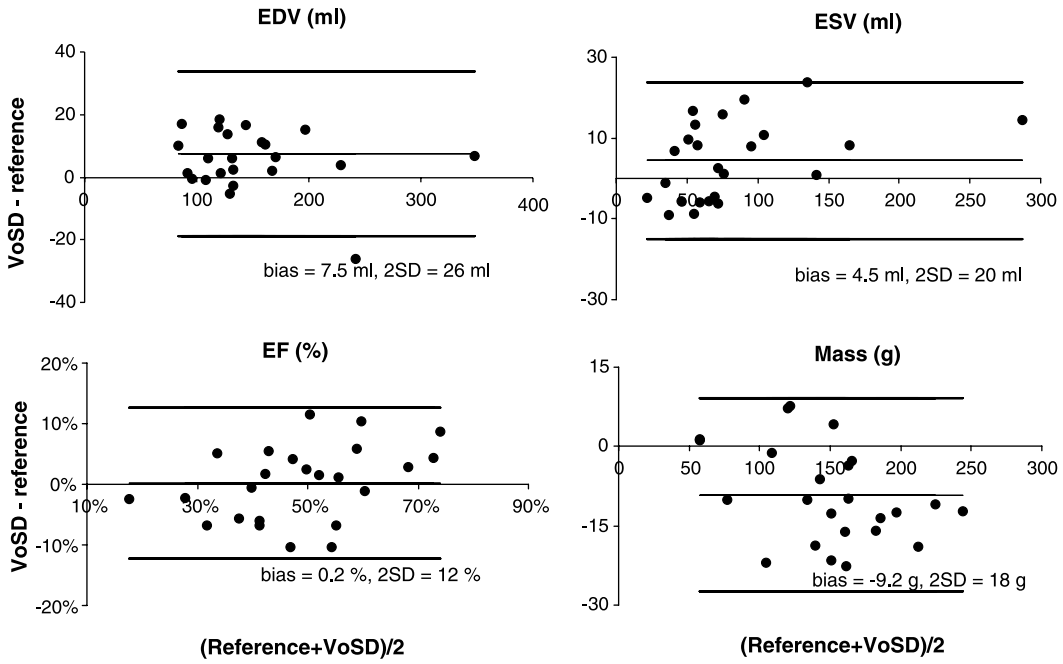

Figure 5. Bland-Altman analysis for LV EDV, ESV, EF and mass obtained by the VoSD technique compared to the standard reference technique.

in percent of their mean. Similarly, inter-observer variability of both techniques was calculated for each measured parameter as the absolute difference between the measurements performed by the two investigators in percent of their mean. For both inter- and intra-observer variability of each parameter, paired *t*-test was used to test the significance of the differences between the two techniques.

3. Results

All patients had normal sinus rhythm and a mean heart rate of 71 bpm (range: 50–115 bpm). Image acquisition lasted between 10 and 15 sec depending on heart rate, respiration rate, and the quality of ECG signal in each patient. End-diastolic and end-systolic volumes measured from conventional semi-automated tracings ranged widely from 78 to 345 mL and from 24 to 280 mL, respectively, reflecting the inhomogeneity of the study group. Accordingly, EF also ranged widely from 19 to 71% and mass from 57 to 245 g. The analysis of a single dataset using the reference technique required between 10 and 20 minutes. In contrast, the VoSD analysis including data retrieval, frame selection, surfaces initialization, and computation of volumes and mass were completed in every patient in less than 5 minutes on a personal computer (Pentium II, 755MHz, 512Mb RAM).

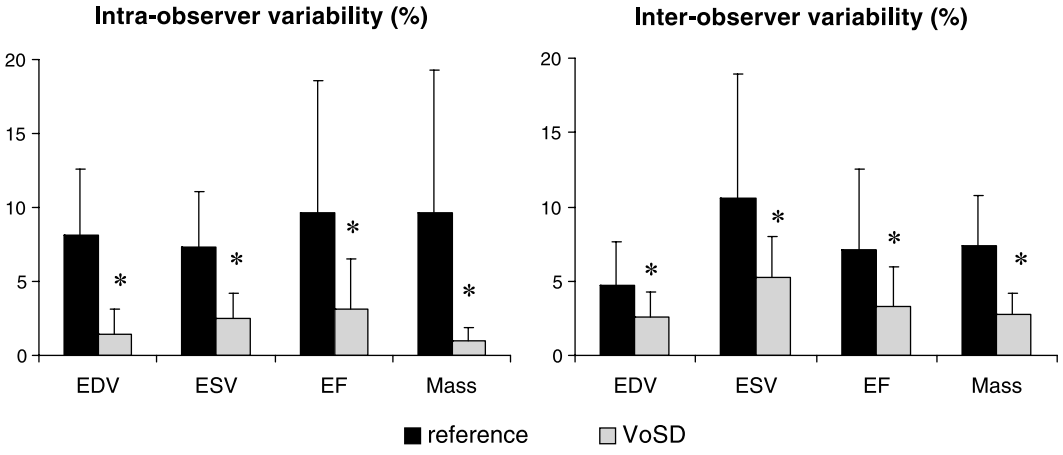

Figure 6. Intra-observer (left) and inter-observer (right) variability of the VoSD technique and the standard reference technique calculated for LV EDV, ESV, EF and mass ($p < 0.05$).

Linear regression analysis (Fig. 4) between the VoSD and the reference volume values resulted in high correlation coefficients and regression slopes near 1.0 for both end-diastolic and end-systolic volumes (EDV: $r = 0.98$, $y = 0.95x + 15$; ESV: $r = 0.99$, $y = 1.06x - 0.5$). Excellent correlations were observed also for LV ejection fraction (EF: $r = 0.91$, $y = 1.08x - 0.04$) and LV mass ($r = 0.98$, $y = 0.91x + 4.6$).

Bland-Altman analysis (Fig. 5) showed no significant biases between the VoSD measurements and the reference technique for EDV, ESV and EF (bias: 7.5 ml; 4.5 ml and 0.2%, respectively), as well as LV mass (bias: −9.2 g). These biases reflected systematic errors of 5.0%, 5.5%, 0.5% and −6.2% of the corresponding mean values. The 95% limits of agreement were relatively narrow (EDV: 26 ml, ESV: 20 ml, EF: 12%, mass: 18 g), providing additional support to the tight agreement between the two techniques.

Figure 6 presents the calculated intra- and inter-observer variability values for the VoSD and the standard reference techniques for EDV, ESV, EF, and mass. The intra-observer variability ranged from 7 to 10% for the standard reference technique and only 1 to 3% for the VoSD technique. This three-fold difference was found statistically significant for all measured parameters. The inter-observer variability ranged from 5 to 11% for the standard reference technique and only 3 to 5% for the VoSD technique, which was also significantly different for all parameters.

4. Discussion

CMRI provides accurate measurements of LV volumes and mass in different patient populations (1, 2, 8). Nevertheless, the quantification of volumes is based on time-consuming manual or semi-automated tracing of endo- and epicardial boundaries in multiple slices. The subjective nature of this procedure limits the reproducibility of volume measurements (2). Additionally, the use of disk approximation in slices where the endocardium is not perpendicular to the imaging plane may introduce errors that are more significant when slices are thick relative to the LV cavity cross-sectional area. Moreover, volume measurements may also be biased by the use of a fixed number of slices of fixed thickness throughout the cardiac cycle in slices where endocardial motion is not limited to the imaging plane. This is because during different phases of the cardiac cycle, a fixed plane contains different anatomic slices of the ventricle rather than reflects the true endocardial motion in a single slice.

The technique we developed overcomes these limitations by directly calculating LV volumes from endo- and epicardial surfaces detected in 3D space without any a priori knowledge of the LV shape and without the use of geometric modeling. Surface modeling from 3D data has been used by several previous investigators (8). In a recent paper, a surface model optimization was applied to 3D echocardiographic images, based on integration of the low level image evidence and the high level prior shape knowledge in a Bayesian framework (9). This model is completely free of geometric modeling but still relies on the priori knowledge of the LV shape. To build a 3D surface not based on the a priori knowledge of the LV shape, we used for surface detection the level-set approach (4–6), which has been previously shown to successfully provide image segmentation in the presence of complex morphology and topological variations. This approach has been applied to different types of medical images including cardiac ultrasound (7, 10–13) and magnetic resonance (11, 14–18). However, to the best of our knowledge, the use of the 3D level-set methods without a priori shape knowledge or geometric modeling for the assessment of LV volumes and mass from cardiac CMRI has not been described previously, and this study represents the first attempt to test the clinical applicability of this methodology in this context. The results of this study proved the feasibility of using the level-set approach for accurate and reproducible evaluation of LV volumes, EF, and mass.

In a previous study, Young et al. described a technique for endocardial and epicardial surface detection (19), based on a general finite element model of the left ventricle, which is represented by an ellipsoid and scaled to each heart according to the distance from base to apex. This model is then modified according to guide-points placed by the user. The fitting of the model to the guide-points is performed by minimizing an error function consisting of the sum of a smoothing term and a term penalizing the distance between each guide-point and the corresponding model position. This procedure results in two models representing the endocardium and the epicardium. From these models, the volumes are computed by applying the same geometric modeling utilized to compute volumes from manual contours. In contrast, with our approach, no priori knowledge of the shape of the left ventricle is necessary. Instead, the operator selects a small number of points from which a rough ventricular shape is computed and successively refined by repeatedly applying the partial differential equation. For both methods, the time of analysis and the level of user interaction are comparable, and an improvement with respect to manual contouring is similar. However, the significant difference between observers described by Young et al. points at the subjective nature of their technique. In this approach, the subjective influences of the manual surface initialization are likely to be "forgotten" during surface evolution by the time stable solution is reached.

A limitation of the current implementation of the VoSD technique is that it requires manual initialization of endo- and epicardial boundaries. Although this initialization procedure is relatively quick and simple, its subjective nature accounts for the non-zero inter-measurement variability of this technique as a whole. A fully automated technique for border initialization would circumvent this limitation. Such fully automated techniques are indeed available in standard commercial analysis software packages and could be used

instead of the manual initialization. While these commercial techniques do not always provide perfect boundary detection without manual adjustments, they may provide sufficient information for the boundary initialization. In this study, we did not use commercial software for initialization because commercial software does not allow exporting the boundaries for further processing. Integrating existing techniques or newer sophisticated algorithms for fully automated boundary initialization (20) with the VoSD technique is likely to lead to even more accurate and reproducible evaluation of LV function and mass from CMRI data.

A limitation of this study was the exclusion of basal slices that contained the LV outflow tract, in which the definition of LV boundaries is most subjective. Including these slices would require additional user input and would likely have further increased the levels of inter-measurement variability for both techniques, the standard reference, and VoSD. Since the extent of this increase in variability cannot be estimated based on our results, the potential need to include these challenging slices will require further development and testing of appropriate algorithms.

Another limitation of this study is that the VoSD technique was not tested in different specific patient populations. Of particular interest would be to establish normal values for this new technique. This was not done because we studied a group of 24 unselected patients of whom only 6 had normal LV size and function, and we felt that it would be inappropriate to claim that values obtained in this small subgroup of subjects could reliably represent normal values of the general population. However, the high levels of agreement between VoSD technique and standard reference values suggest that the normal values should not be different from those previously established. Nevertheless, our goal of testing the feasibility and validating our newly developed technique in a wide range of conditions was achieved by enrolling unselected patients representing a variety of cardiac disease states. The results of this study warrant future studies geared toward further validation of our technique in more narrowly defined patient populations.

Despite these limitations, these results showed that this new technique is accurate since it provided LV volume, EF, and mass values in close agreement with the standard reference technique. Since this reference technique is widely considered the ''gold standard'' for these measurements, it is difficult to directly prove that a new technique could be more accurate. Nevertheless, the VoSD approach was found to be more reproducible than the conventional methodology. Importantly, the levels of inter- and intra-observer variability of the latter technique measured in our study was similar to those reported by several previous investigators (21). Sakuma and colleagues showed in normal subjects an inter-observer variability of 4 and 8% for EDV and ESV, respectively (22); other reports included intra- and inter-observer variability of 2 to 7% and 3.6 to 7.3%, respectively (23). A third report provided 1.6 to 6.6% and 1.6 to 7.3%, respectively (24), for intra- and inter-observer variability. Similar results were reported for heart failure patients (24, 25). The intra-observer and inter-observer variability and the negligible biases of the VoSD technique support the hypothesis that this technique could result in improvement in diagnostic accuracy. In addition, this technique is faster even in its current version, since the interactive part of the procedure only consists of the initialization of a small number of points in a few planes.

Moreover, theoretically, this approach could allow automated, full temporal analysis of the LV volume by using the detected surface of each frame as the initial condition for the following frame throughout the cardiac cycle. Thus, manual interaction would only be necessary for the first frame analyzed. Importantly, considering that of the 5 minutes necessary to analyze a single dataset, surface evolution takes only 30 sec, and analysis of all phases of the cardiac cycle would only add 30 sec times the number of frames, i.e. less than 10 min, which could be further reduced by using a more powerful computer.

Other potential future applications of this approach may include the evaluation of right ventricular function, which today requires tedious frame-by-frame manual tracing and is known to be challenging because the morphology of this chamber is complex, irregular, and widely variable between subjects (26, 27). The main advantage of VoSD technique in this context is that it requires no priori knowledge or modeling of the chamber geometry. Therefore, this approach may allow easier and more accurate assessment of the right ventricle (28).

In summary, this study proved the clinical feasibility of level-set volumetric surface detection from cardiac MR images geared toward the assessment of LV performance. The results of this validation study demonstrated that the proposed method allows rapid and accurate measurements of LV volumes, EF, and mass, in agreement with conventional semi-automated tracing with the advantage of being fast and independent of geometrical assumptions or modeling. Importantly, the improved reproducibility of this new technique indicates a potential accuracy advantage over the current standard reference methodology.

References

1. Dulce MC, Friese K, Albrecht A, Hamm B, Buttner P, Wolf KJ. Variability and reproducibility in the determination of left-ventricular heart volume by cine-MR. A comparison of measurement methods. Rofo 1991; 155:99–108.
2. Pattynama PM, Lamb HJ, Van der Velde EA, van der Wall EE, De Roos A. Left ventricular measurements with cine and spin-echo MR imaging: a study of reproducibility with variance component analysis. Radiology 1993; 187:261–268.
3. Thiele H, Paetsch I, Schnackenburg B, Bornstedt A, Grebe O, Wellnhofer E, Schuler G, Fleck E, Nagel E. Improved accuracy of quantitative assessment of left ventricular volume and ejection fraction by geometric models with steady-state free precession. J Cardiovasc Magn Reson 2002; 4:327–339.

4. Osher S, Sethian JA. Fronts propagating with curvature-dependent speed—algorithms based on Hamilton-Jacobi formulations. J Comput Phys 1988; 79:12–49.
5. Malladi R, Sethian JA, Vemuri BC. Shape modeling with front propagation—a level set approach. IEEE Trans Pattern Anal Mach Intell 1995; 17:158–175.
6. Sethian JA. Level Set Methods and Fast Marching Methods. Cambridge: Cambridge University Press, 1999.
7. Corsi C, Saracino G, Sarti A, Lamberti C. Left ventricular volume estimation for real-time three-dimensional echocardiography. IEEE Trans Med Imag 2002; 21:1202–1208.
8. Frangi AF, Niessen WJ, Viergever MA. Three-dimensional modeling for functional analysis of cardiac images: a review. IEEE Trans Med Imag 2001; 20:2–25.
9. Song M, Haralick RM, Sheehan FH, Johnson RK. Integrated surface model optimization for freehand three-dimensional echocardiography. IEEE Trans Med Imag 2002; 21:1077–1090.
10. Sarti A, Mikula K, Sgallari F. Nonlinear multiscale analysis of three-dimensional echocardiographic sequences. IEEE Trans Med Imag 1999; 18:453–466.
11. Chen YM, Guo WH, Huang F, Wilson D, Geiser EA. Using prior shape and points in medical image segmentation. Energy Minim Methods Comput Vis Pattern Recogn, Proc 2003; 2683:291–305.
12. Lin N, Yu W, Duncan JS. Combinative multi-scale level set framework for echocardiographic image segmentation. Med Image Anal 2003; 7:529–537.
13. Deschamps T, Malladi R, Ravve I. Fast evolution of image manifolds and application to filtering and segmentation in 3D medical images. IEEE Trans Vis Comput Graph 2004; 10:525–535.
14. Chen YM, Tagare HD, Thiruvenkadam S, Huang F, Wilson D, Gopinath KS, Briggs RW, Geiser EA. Using prior shapes in geometric active contours in a variational framework. Int J Comput Vis 2002; 50:315–328.
15. Kaus MR, von Berg J, Niessen W, Pekar V. Automated segmentation of the left ventricle in cardiac MRI. Medical Image Computing and Computer-Assisted Intervention—Miccai 2003. 2003; 2878(pt 1): 432–439.
16. Lorenzo-Valdes M, Sanchez-Ortiz GI, Mohiaddin R, Rueckert D. Segmentation of 4D cardiac MR images using a probabilistic atlas and the EM algorithm. Medical Image Computing and Computer-Assisted Intervention—Miccai 2003. 2003; 2878(pt 1): 440–450.
17. Paragios N. A level set approach for shape-driven segmentation and tracking of the left ventricle. IEEE Trans Med Imag 2003; 22:773–776.
18. Yang J, Staib LH, Duncan JS. Neighbor-constrained segmentation with level set based 3-D deformable models. IEEE Trans Med Imag 2004; 23:940–948.
19. Young AA, Cowan BR, Thrupp SF, Hedley WJ, Dell'Italia LJ. Left ventricular mass and volume: fast calculation with guide-point modeling on MR images. Radiology 2000; 216:597–602.
20. van der Geest RJ, Lelieveldt BP, Angelie E, Danilouchkine M, Swingen C, Sonka M, Reiber JH. Evaluation of a new method for automated detection of left ventricular boundaries in time series of magnetic resonance images using an Active Appearance Motion Model. J Cardiovasc Magn Reson 2004; 6:609–617.
21. Myerson SG, Bellenger NG, Pennell DJ. Assessment of left ventricular mass by cardiovascular magnetic resonance. Hypertension 2002; 39:750–755.
22. Sakuma H, Fujita N, Foo TK, Caputo GR, Nelson SJ, Hartiala J, Shimakawa A, Higgins CB. Evaluation of left ventricular volume and mass with breath-hold cine MR imaging. Radiology 1993; 188:377–380.
23. Bogaert JG, Bosmans HT, Rademakers FE, Bellon EP, Herregods MC, Verschakelen JA, Van de WF, Marchal GJ. Left ventricular quantification with breath-hold MR imaging: comparison with echocardiography. Magma 1995; 3:5–12.
24. Bellenger NG, Davies LC, Francis JM, Coats AJ, Pennell DJ. Reduction in sample size for studies of remodeling in heart failure by the use of cardiovascular magnetic resonance. J Cardiovasc Magn Reson 2000; 2:271–278.
25. Matheijssen NA, Baur LH, Reiber JH, van d, V, van Dijkman PR, van der Geest RJ, de RA, van der Wall EE. Assessment of left ventricular volume and mass by cine magnetic resonance imaging in patients with anterior myocardial infarction intra-observer and inter-observer variability on contour detection. Int J Card Imaging 1996; 12:11–19.
26. Grothues F, Moon JC, Bellenger NG, Smith GS, Klein HU, Pennell DJ. Interstudy reproducibility of right ventricular volumes, function, and mass with cardiovascular magnetic resonance. Am Heart J 2004; 147:218–223.
27. Pattynama PM, Lamb HJ, Van der Velde EA, van der Geest RJ, van der Wall EE, De Roos A. Reproducibility of MRI-derived measurements of right ventricular volumes and myocardial mass. Magn Reson Imaging 1995; 13:53–63.
28. Battani R, Corsi C, Sarti A, Lamberti C, Piva T, Fattori R. Estimation of right ventricular volume without geometrical assumptions utilizing cardiac magnetic resonance data. Comput Cardiol 2003; 30:81–84.